Alignment and Imaging of the CS_2 Dimer Inside Helium Nanodroplets

James D. Pickering, Benjamin Shepperson, Bjarke A. K. Hübschmann, Frederik Thorning, and Henrik Stapelfeldt*
Department of Chemistry, Aarhus Univeristy, Langelandsgade 140, 8000 Aarhus C, Denmark

(Received 9 November 2017; published 13 March 2018)

The carbon disulphide (CS_2) dimer is formed inside He nanodroplets and identified using fs laser-induced Coulomb explosion, by observing the CS_2^+ ion recoil velocity. It is then shown that a 160 ps moderately intense laser pulse can align the dimer in advantageous spatial orientations which allow us to determine the cross-shaped structure of the dimer by analysis of the correlations between the emission angles of the nascent CS_2^+ and S^+ ions, following the explosion process. Our method will enable fs time-resolved structural imaging of weakly bound molecular complexes during conformational isomerization, including formation of exciplexes.

DOI: 10.1103/PhysRevLett.120.113202

Complexes of molecules and/or atoms held together by weak noncovalent interactions are ubiquitous in the natural sciences. Examples are wide ranging, from exotic quantum halos, such as He_2 [1,2] and HeLi [3], characterized by extremely small binding energies, to pairs of aromatic molecules where their mutual interaction plays an important role for the stabilization of protein structures [4]. Many studies have focused on gas-phase complexes, notably van der Waals (VDW) dimers, created by supersonic expansion of gases into vacuum. Microwave, infrared and ultraviolet spectroscopy have been combined with theoretical calculations to give detailed structural information for a wide variety of species [5–7]. An important insight is that VDW dimers can provide well defined initial conditions for studying intermolecular processes such as excimer or exciplex formation [8] and bimolecular reactions [9]. An intriguing possibility, not offered by frequency-resolved spectroscopy, is to image the structure of such molecular complexes during conformational changes. This requires a method capable of imaging the structure with fs time resolution.

Here we apply Coulomb-explosion imaging (CEI) triggered by an intense fs laser pulse to determine the structure of a VDW bonded molecular dimer. Specifically, by fixing the molecular frame of CS_2 dimers in space, using laser-induced alignment [10], we show that by observing and correlating the recoil velocities of the ion fragments, we are able to determine critical bond angles of the dimer and thereby the overall structure. This marks a significant step forward, compared to previous works, where CEI was applied to complexes up to the size of a diatomic molecule bound to an atom [11,12]. Furthermore, our studies go beyond previous works by being conducted on dimers embedded in helium nanodroplets. The prime advantage of this is the much larger variety and better control of complexes produced in He droplets when compared to those produced in gas-phase supersonic expansions [13–15]. In addition, the 0.38 K rotational temperature imposed by the helium environment ensures a very high degree of alignment [16], which is beneficial for extracting maximum structural information.

The experimental setup has been described in detail before [16], and only a few important aspects will be pointed out (see Fig. 1). A beam of He droplets is formed by continuously expanding He gas at 16 K and 30 bar backing pressure into vacuum through a 5 μm nozzle. The droplets, consisting of 8000 He atoms on average [17], are passed through a pickup cell containing CS_2 vapor. The probability for the droplets to pick up one or two CS_2 molecules depends on the partial pressure of CS_2 in the cell. As discussed below, this allows us to control the formation

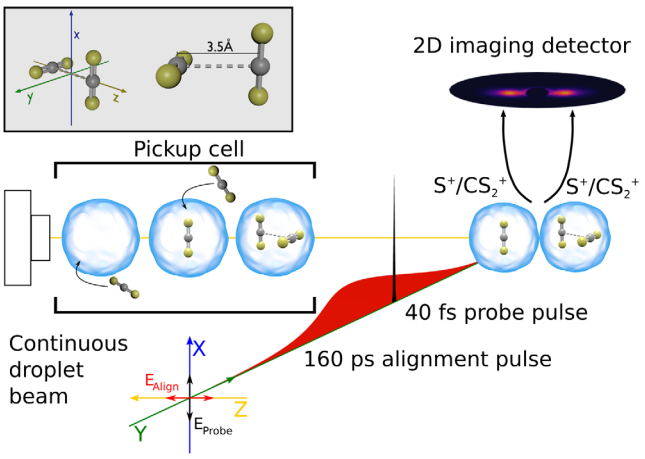

FIG. 1. Schematic of the key elements in the experiment. In the case depicted here, the alignment (probe) laser pulse is linearly polarized along the Z axis (X axis). The electrostatic plates of the VMI spectrometer projecting the CS_2^+ or S^+ ions onto the imaging detector are not shown. The inset shows a sketch of the gas-phase dimer structure.

of CS_2 dimers inside the He droplets. The doped droplet beam enters the interaction region where it is crossed by two focussed laser beams both originating from the same Ti-Sapphire laser system. One beam, consisting of 160 ps (FWHM) pulses ($\lambda_{\text{center}} = 800$ nm, $I_0 = 8 \times 10^{11}$ W/cm^2), is used to align the solvated molecules. The second beam, consisting of 40 fs probe pulses ($\lambda_{\text{center}} = 800$ nm, $I_0 = 3 \times 10^{14}$ W/cm^2), is used to (multiply) ionize the molecules in order to both identify the formation of CS_2 dimers and determine their alignment and molecular structure. This is based on detection of the nascent CS_2^+ and S^+ ions using a velocity-map imaging spectrometer and 2D imaging detector backed by a CCD camera. The experiments are run at the 1 kHz repetition rate of the laser system.

A sketch of the molecular structure of the CS_2 dimer in the gas-phase, determined by IR spectroscopy [18], is displayed in Fig. 1 (inset). The two CS_2 monomers are connected in a cross-shaped geometry and the *C-C* distance is 3.5 Å; i.e., it is a prolate symmetric top with D_{2d} symmetry. According to a DFT calculation (wb97xd/aug-pcseg-2) the polarizability components for the dimer are: $\alpha_{xx} = \alpha_{yy} = 17.5$ Å^3, $\alpha_{zz} = 12.0$ Å^3 (see Supplemental Material [19], which includes Refs. [20,21]), where the z axis is parallel to the *C-C* axis and the x axis and y axis are parallel to each of the monomer axes. To our knowledge the CS_2 dimer has never been studied in He droplets.

First, we demonstrate that it is possible to form and detect CS_2 dimers inside the He droplets. The detection is done by measuring the velocity of the CS_2^+ ions created by the probe pulse. If a droplet contains a single CS_2 molecule, the resulting CS_2^+ ion will emerge with very low kinetic energy [22]; whereas if a droplet contains a CS_2 dimer and both monomers are ionized, the CS_2^+ ions acquire kinetic energy due to their mutual Coulomb repulsion. Double ionization of a dimer should be thought of as the ionization of each of its two individual CS_2 molecules independently. Single ionization of a CS_2 molecule was saturated at the probe intensity used. Therefore, we expect that the probability for double ionization of a dimer is essentially the same as for single ionization of a CS_2 molecule.

Figure 2(a1) shows a velocity image of CS_2^+ ions recorded with the probe pulse only, polarized perpendicular to the detector. The image is dominated by an intense signal in the central portion, corresponding to low kinetic energy of the CS_2^+ ions. Therefore, we assign this signal to ionization of CS_2 monomers in droplets doped with a single molecule. There is also a significant amount of signal detected at larger radii, corresponding to larger kinetic energies, which is consistent with ionization of both CS_2 molecules in droplets doped with a dimer [23]. To substantiate this assignment we calculated the angular covariance map [25,26], Fig. 2(a2), from ions in the radial range outside of the annotated yellow circle. Two distinct

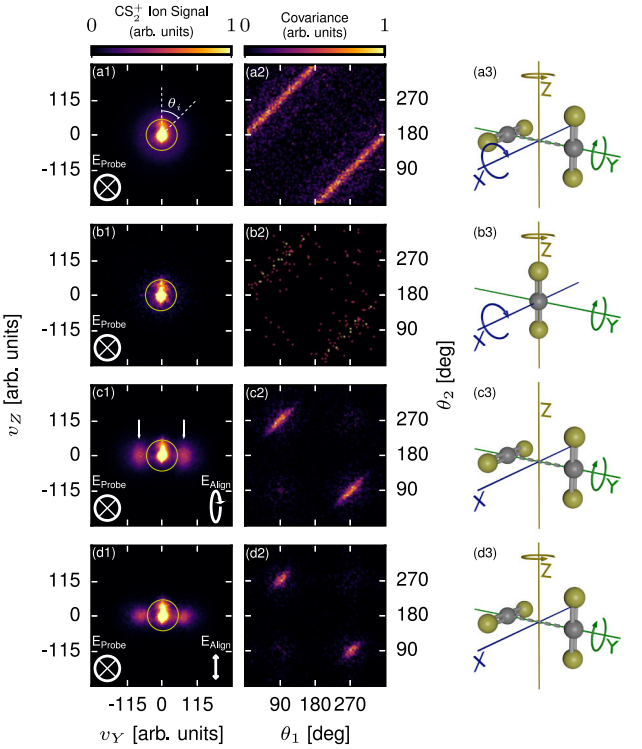

FIG. 2. (a1)–(d1) CS_2^+ ion images and (a2)–(d2) corresponding angular covariance maps created from ions outside the yellow circles. The polarization state of the probe (alignment) pulse is given in the lower left (right) corner of each ion image. Data in rows (a),(c),(d) [(b)] were recorded for the dimer-[monomer-] doping condition. (a3)–(d3) illustrate the spatial alignment of the monomer or dimer derived from the ion images and covariance maps (see text), curved arrows indicate axes about which there is free rotation.

diagonal lines centered at $\theta_2 = \theta_1 - 180°$ and $\theta_2 = \theta_1 + 180°$ stand out and show that the emission direction of a CS_2^+ ion is correlated with another CS_2^+ ion departing in the opposite direction [θ_i, $i = 1,2$ is the angle between an ion hit and the vertical center line, see Fig. 2(a1)]. This strongly indicates that the ions originate from ionization of both CS_2 molecules in dimer-containing droplets and subsequent fragmentation into a pair of CS_2^+ ions. Therefore, we interpret the angular positions of the CS_2^+ ion hits outside the yellow circle as a measure of the (projected) emission directions of the CS_2^+ ions from dimers. This is a measure of the spatial orientation of the *C-C* axes in the dimers at the instant of ionization. The uniform extent of the covariance signal over 360° shows that the *C-C* axes are randomly oriented, illustrated in Fig. 2(a3), which is expected in the absence of an alignment pulse.

Figure 2(b1) displays a similar CS_2^+ image but using a lower CS_2 partial pressure. It appears that there are now relatively fewer ions detected outside compared to inside the yellow circle [19]. In addition, the diagonal lines in the angular covariance map, Figure 2(b2), have almost

disappeared showing that there are very few dimers present under these doping conditions. This will be called the monomer-doping condition, whereas the condition used for recording the data in Fig. 2(a) will be referred to as the dimer-doping condition. Note, however, that in this regime there are still more droplets doped with monomers than with dimers [17].

Next, we demonstrate that it is possible to align the CS_2 dimers in the He droplets and exploit this to show that their structure is cross shaped. For these experiments, the dimer-doping condition is used and the alignment pulse is included. With its 160 ps duration, the alignment dynamics is expected to be essentially adiabatic. Therefore, the probe pulse is synchronized to the peak of the alignment pulse where the alignment should be strongest [16]. First, a circularly polarized alignment pulse is used. Figure 2(c1) shows that in this case the emission direction of the CS_2^+ ions outside the yellow circle is strongly confined along the Y axis and the correlation signals in the covariance map, Fig. 2(c2), are truncated to short islands centered at (90°, 270°) and (270°, 90°). In addition, the radial distribution outside the yellow circle is peaked at the outermost part, marked by white arrows, and separated from the major signal in the center. These observations demonstrate that the CS_2 dimers are aligned with the C-C axis confined along the Y axis. A circularly polarized alignment field confines the least polarizable molecular axis perpendicular to the polarization plane [27] (along the Y axis, see Fig. 1). Consequently, the dimer inside the He droplets must have a structure where the C-C axis is the least-polarizable axis. This is the case for a cross shape, as that of the gas-phase dimer, but not for a T shape, or a slipped-parallel shape [19]. Therefore, we conclude that the dimer is cross shaped and aligned, as shown in Fig. 2(c3). The dihedral angle between the two monomer axes cannot be determined from detecting CS_2^+ ions, but below we show that this is possible from images of S^+ ions.

For a linearly polarized alignment pulse, polarized along the Z axis, the ejected CS_2^+ ions are also confined along the Y axis [Fig. 2(d1)], and again, the covariance map contains short islands centered at (90°, 270°) and (270°, 90°)—see Fig. 2(d2). As discussed in [19], these observations show that the C-C axis is aligned perpendicular to, and free to rotate around, the polarization (Z) axis as illustrated in Fig. 2(d3).

Finally, we demonstrate how the dihedral angle between the CS_2 monomers in the dimer can be determined by analyzing S^+ ion images and, in particular, the corresponding angular covariance maps. Figure 3(a1) shows an S^+ ion image recorded with a linearly polarized alignment pulse, polarized along the Z axis, for the monomer-doping condition. The S^+ ions are confined along the vertical (Z) axis in the image demonstrating 1D alignment of the CS_2 molecules similar to that observed previously for other molecules in He droplets [16,28]. The covariance map,

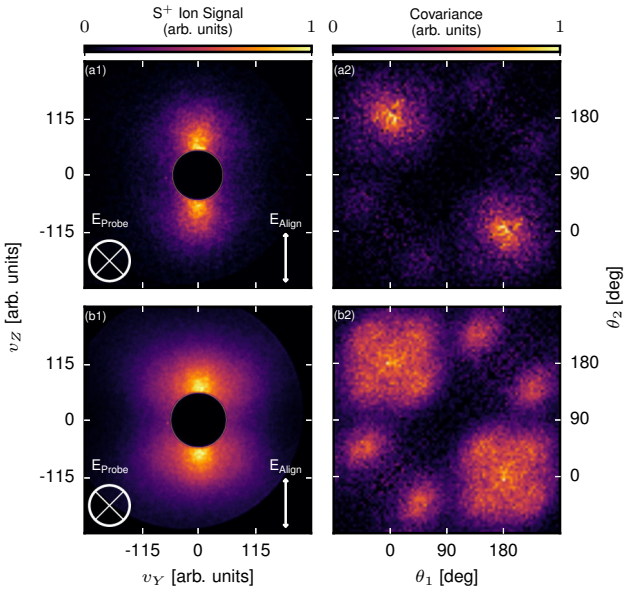

FIG. 3. (a1)–(b1) S^+ ion images and (b1)–(b2) corresponding angular covariance maps created from ions outside the yellow circles. The polarization state of the probe (alignment) pulse is given in the lower left (right) corner of each ion image. Image (a) [(b)] was recorded under the monomer-[dimer]-doping condition. Here, the central region is removed due to background contaminants occurring at $m/z = 32$ Da.

Fig. 3(a2), reveals pronounced correlation between S^+ ions detected at 0° and 180°. This shows that the probe pulse causes at least double ionization of the CS_2 molecules and, in the subsequent fragmentation of the ionized molecules, two S^+ ions departing along the internuclear axis in opposite directions [29].

Figure 3(b1) displays the S^+ ion image recorded for the dimer-doping condition. As in panel 3(a1), the ions are localized around the polarization of the alignment pulse but the angular distribution is broader. The contribution from the dimer-doped droplets stands out most clearly in the angular covariance map, Fig. 3(b2). In addition to the prominent monomer signals at (0°, 180°) and (180°, 0°), strong correlations are present, centered approximately at (−45°, 45°), (−45°, 135°), (−45°, 225°), (45°, 135°), (45°, 225°), (135°, 225°), and since the covariance map is an autovariance map, at six equivalent positions obtained by mirroring in the central diagonal.

Row (a) in Fig. 4 is a schematic of three different dimer orientations, imposed by the alignment pulse, as seen in perspective. The dimers are sketched for a 90° dihedral angle between the CS_2 monomers. Row (b) shows the resulting S^+ ion emission directions onto the detector (YZ) plane assuming recoil along the parent C—S bonds. If the dimer is oriented as in Fig. 4(a1), the S^+ ions would recoil at angles of −45°, 45°, 135°, and 225°, with respect to the upwards vertical. This would exactly create the 2×6 correlation islands present in the angular covariance

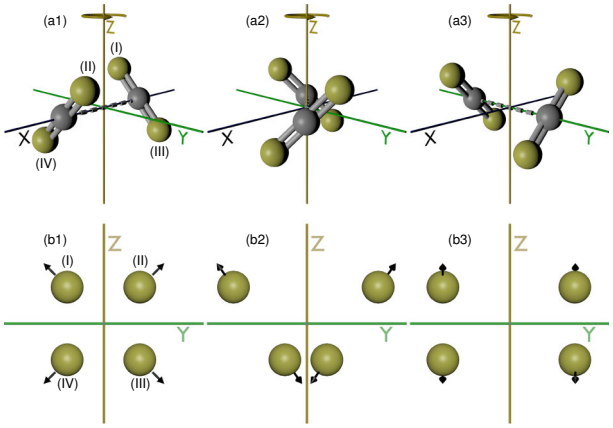

FIG. 4. (a1)–(a3): Detector view of the dimer for three rotation angles, α, around the alignment polarization axis (Z axis). (b1)–(b3): The velocities of the corresponding S^+ ions in the detector (YZ) plane.

map, Fig. 3(b2). To understand why other dimer orientations also lead to these 2×6 correlation islands, we first note that the linearly polarized alignment pulse places the C-C axis perpendicular to the Z axis [see Fig. 2(d3)]. The three dimer orientations in Fig. 4 are depicted for α equal to 0°, 45°, and 90°, where α is the angle between the X axis and the C-C axis. The detector records the projection of the angle between the S^+ ion recoil directions and only in panel (a1) does this correspond to the true angle between the C—S bonds in the parent dimer. Concentrating on the projected angle, termed β, between the C—S(I) and the C—S(II) bonds geometrical considerations establish that [19]:

$$\cos\beta = \frac{\sin^2\alpha}{1+\cos^2\alpha}. \quad (1)$$

There is free rotation of the C-C axis around the Z axis so α is randomly distributed over its 360° interval. Equation (1) then shows that the probability density of β is strongly peaked at 90° [19]; it is much more likely for the projected angle to be near 90° than near 0°. This explains why the correlations are localized at (45°, −45°) and (−45°, 45°), rather than extending as a uniform band from (45°, −45°) to (−45°, 45°). The faint signal in the band between these two correlation areas indicate that projected angles less than 90° are possible but unlikely. Similar arguments can be used to explain the localization of the other 2×5 correlation islands.

A crucial question that remains to be answered is why the CS_2 monomers of the dimer are aligned at 45° to the alignment polarization (along the Z axis), as illustrated in Fig. 4(a1). If the angle between the CS_2 monomers in the dimer is 90°, used for the sketches in Fig. 2 and Fig. 4, there should be free rotation around the C-C axis due to uniform polarizability in the molecular xy plane. This would create correlation stripes extending over 360° in the covariance map—for instance a stripe centered around $\theta_2 = \theta_1 + 90°$—at odds with the three localized islands observed at (−45°,45°), (45°,135°), and (135°, 225°). The explanation, we believe, is that the angle between the CS_2 monomers deviates from 90°. The deviation is caused by the alignment field, which tries to align each of the CS_2 monomers along its polarization axis. The torsional potential resulting from the interaction between the two monomers prevents this from happening, and instead, the monomers settle at an equilibrium angle, less than 90°, determined by the minimum in the sum of the inherent torsional potential and the laser-induced alignment potential.

A deviation from 90° should manifest itself in the covariance islands in Fig. 3(b2). We analyzed the (−45°, 45°) and the (135°, 225°) islands and found that they are centered at (−39°,45°) and (137°,222°) [19]. This corresponds to 84° and 85° for the angle between the monomers. Consequently, the (−45°, −225°) and (45°, 135°) covariance islands should show an equivalent increase in the dihedral angle by 5°. Unfortunately, the strong covariance signal centered at (0°,180°) extends so much that it blurs the (−45°, 225°) and (45°,135°) signals to an extent that their centers cannot be reliably determined. Although the mild distortion does not impair the ability to extract structural information, we believe it can be eliminated by using field-free alignment through rapid truncation of the alignment pulse [30]. Furthermore, the distortion effect may be exploited for inducing and directly imaging torsion of the monomers in real time [25,31].

We have shown that the structure of molecular dimers in He droplets can be determined by combining fs laser-induced Coulomb explosion and laser-based molecular alignment. For the CS_2 dimer studied here, as an example, the structure was found to be 90° cross shaped, similar to the minimum energy configuration observed in gas-phase. Gas phase calculations predict other stable, higher energy, configurations like the slipped-parallel structure [18]. We saw no indication of this configuration, but note that, for other molecules, notably HCN [32], it has been observed that dimers, and larger oligomers, get trapped in local energy minima due to the annealing effect of the He environment. The ability of CEI to determine absolute structures will typically not match that available through frequency-resolved spectroscopy—at least not for small molecules. The critical aspect of our method is, however, that it will enable fs time-resolved imaging of molecular structure during isomerization (for example exciplex formation) [33,34] and bimolecular reactions [35], by initiating the dynamics from prereactive complexes with a fs pump pulse. The possibility to now do this in He droplets points towards studies on a variety of species not accessible by gas-phase methods.

We acknowledge support from the European Research Council-AdG (Project No. 320459, DropletControl) and from the European Union Horizon 2020 research and

innovation program under the Marie Sklodowska-Curie Grant Agreement No. 641789 MEDEA. We thank Frank Jensen for theoretical support. J. P. thanks Michael Burt for useful discussions.

*henriks@chem.au.dk

[1] R. E. Grisenti, W. Schollkopf, J. P. Toennies, G. C. Hegerfeldt, T. Kohler, and M. Stoll, Determination of the Bond Length and Binding Energy of the Helium Dimer by Diffraction from a Transmission Grating, Phys. Rev. Lett. **85**, 2284 (2000).

[2] S. Zeller, M. Kunitski, J. Voigtsberger, A. Kalinin, A. Schottelius, C. Schober, M. Waitz, H. Sann, A. Hartung, T. Bauer, M. Pitzer, F. Trinter, C. Goihl, C. Janke, M. Richter, G. Kastirke, M. Weller, A. Czasch, M. Kitzler, M. Braune, R. E. Grisenti, W. Schöllkopf, L. Ph. H. Schmidt, M. S. Schöffler, J. B. Williams, T. Jahnke, and R. Dörner, Imaging the He_2 quantum halo state using a free electron laser, Proc. Natl. Acad. Sci. U.S.A. **113**, 14651 (2016).

[3] N. Tariq, N. A. Taisan, V. Singh, and J. D. Weinstein, Spectroscopic Detection of the LiHe Molecule, Phys. Rev. Lett. **110**, 153201 (2013).

[4] S. K. Burley and G. A. Petsko, Aromatic-aromatic interaction: a mechanism of protein structure stabilization, Science **229**, 23 (1985).

[5] D. J. Nesbitt, High-resolution infrared spectroscopy of weakly bound molecular complexes, Chem. Rev. **88**, 843 (1988).

[6] N. Moazzen-Ahmadi and A. R. W. McKellar, Spectroscopy of dimers, trimers and larger clusters of linear molecules, Int. Rev. Phys. Chem. **32**, 611 (2013).

[7] M. Becucci and S. Melandri, High-resolution spectroscopic studies of complexes formed by medium-size organic molecules, Chem. Rev. **116**, 5014 (2016).

[8] W. T. Yip and D. H. Levy, Excimer/Exciplex formation in van der Waals dimers of aromatic molecules, J. Phys. Chem. **100**, 11539 (1996).

[9] M. D. Wheeler, D. T. Anderson, and M. I. Lester, Probing reactive potential energy surfaces by vibrational activation of $H_2 - OH$ entrance channel complexes, Int. Rev. Phys. Chem. **19**, 501 (2000).

[10] H. Stapelfeldt and T. Seideman, Colloquium: Aligning molecules with strong laser pulses, Rev. Mod. Phys. **75**, 543 (2003).

[11] J. Wu, M. Kunitski, L. Ph. H. Schmidt, T. Jahnke, and R. Dörner, Structures of N_2Ar, O_2Ar, and O_2Xe dimers studied by Coulomb explosion imaging, J. Chem. Phys. **137**, 104308 (2012).

[12] C. Wu, C. Wu, D. Song, H. Su, X. Xie, M. Li, Y. Deng, Y. Liu, and Q. Gong, Communication: Determining the structure of the N_2Ar van der Waals complex with laser-based channel-selected Coulomb explosion, J. Chem. Phys. **140**, 141101 (2014).

[13] M. Y. Choi, G. E. Douberly, T. M. Falconer, W. K. Lewis, C. M. Lindsay, J. M. Merritt, P. L. Stiles, and R. E. Miller, Infrared spectroscopy of helium nanodroplets: novel methods for physics and chemistry, Int. Rev. Phys. Chem. **25**, 15 (2006).

[14] S. Yang and A. M. Ellis, Helium droplets: A chemistry perspective, Chem. Soc. Rev. **42**, 472 (2013).

[15] B. Bellina, D. J. Merthe, and V. V. Kresin, Proton transfer in histidine-tryptophan heterodimers embedded in helium droplets, J. Chem. Phys. **142**, 114306 (2015).

[16] B. Shepperson, A. S. Chatterley, A. A. Søndergaard, L. Christiansen, M. Lemeshko, and H. Stapelfeldt, Strongly aligned molecules inside helium droplets in the near-adiabatic regime, J. Chem. Phys. **147**, 013946 (2017).

[17] J. P. Toennies and A. F Vilesov, Superfluid Helium droplets: A uniquely cold nanomatrix for molecules and molecular complexes, Angew. Chem., Int. Ed. Engl. **43**, 2622 (2004).

[18] M. Rezaei, J. N. Oliaee, N. Moazzen-Ahmadi, and A. R. W. McKellar, Spectroscopic observation and structure of CS_2 dimer, J. Chem. Phys. **134**, 144306 (2011).

[19] See the Supplemental Material at http://link.aps.org/supplemental/10.1103/PhysRevLett.120.113202 for details.

[20] J. Chai and M. Head-Gordon, Long-range corrected hybrid density functionals with damped atom-atom dispersion corrections, Phys. Chem. Chem. Phys. **10**, 6615 (2008).

[21] F. Jensen, Unifying general and segmented contracted basis sets. Segmented polarization consistent basis sets, J. Chem. Theory Comput. **10**, 1074 (2014).

[22] An isolated CS_2 molecule would have (practically) zero velocity after ionization. Inside a He droplet, strong-field ionization of the molecule is typically accompanied by ionization of a few He atoms. We believe the electrostatic interaction with these He^+ ions causes the nonzero velocity of the CS_2^+ ions in the image center.

[23] Some of the kinetic energy is lost due to collisions with He atoms as the CS_2^+ ions travel out of the droplets [24]. Unlike in the gas-phase the kinetic energies detected, therefore, do not immediately provide information on the *C-C* distance.

[24] A. Braun and M. Drabbels, Photodissociation of alkyl iodides in helium nanodroplets. I. Kinetic energy transfer, J. Chem. Phys. **127**, 114303 (2007).

[25] J. L. Hansen, J. H. Nielsen, C. B. Madsen, A. T. Lindhardt, M. P. Johansson, T. Skrydstrup, L. B. Madsen, and H. Stapelfeldt, Control and femtosecond time-resolved imaging of torsion in a chiral molecule, J. Chem. Phys. **136**, 204310 (2012).

[26] C. S. Slater, S. Blake, M. Brouard, A. Lauer, C. Vallance, J. J. John, R. Turchetta, A. Nomerotski, L. Christensen, J. H. Nielsen, M. P. Johansson, and H. Stapelfeldt, Covariance imaging experiments using a pixel-imaging mass-spectrometry camera, Phys. Rev. A **89**, 011401 (2014).

[27] J. J. Larsen, K. Hald, N. Bjerre, H. Stapelfeldt, and T. Seideman, Three Dimensional Alignment of Molecules Using Elliptically Polarized Laser Fields, Phys. Rev. Lett. **85**, 2470 (2000).

[28] D. Pentlehner, J. H. Nielsen, L. Christiansen, A. Slenczka, and H. Stapelfeldt, Laser-induced adiabatic alignment of molecules dissolved in helium nanodroplets, Phys. Rev. A **87**, 063401 (2013).

[29] L. Christiansen, J. H. Nielsen, L. Christensen, B. Shepperson, D. Pentlehner, and H. Stapelfeldt, Laser-induced Coulomb explosion of 1,4-diiodobenzene molecules: Studies of

isolated molecules and molecules in helium nanodroplets, Phys. Rev. A **93**, 023411 (2016).

[30] A. S. Chatterley, C. Schouder, L. Christiansen, M. H. Rasmussen, B. Shepperson, and H. Stapelfeldt, Field-free alignment of large molecules in He nanodroplets (to be published).

[31] L. Christensen, J. H. Nielsen, C. B. Brandt, C. B. Madsen, L. B. Madsen, C. S. Slater, A. Lauer, M. Brouard, M. P. Johansson, B. Shepperson, and H. Stapelfeldt, Dynamic Stark Control of Torsional Motion by a Pair of Laser Pulses, Phys. Rev. Lett. **113**, 073005 (2014).

[32] K. Nauta and R. E. Miller, Nonequilibrium self-assembly of long chains of polar molecules in superfluid helium, Science **283**, 1895 (1999).

[33] M. Miyazaki and M. Fujii, Real time observation of the excimer formation dynamics of a gas phase benzene dimer by picosecond pump-probe spectroscopy, Phys. Chem. Chem. Phys. **17**, 25989 (2015).

[34] H. Saigusa and E. C. Lim, Picosecond photodissociation study of the excimer formation in van der Waals dimers of aromatic molecules, Chem. Phys. Lett. **336**, 65 (2001).

[35] D. Zhong, P. Y. Cheng, and A. H. Zewail, Bimolecular reactions observed by femtosecond detachment to aligned transition states: Inelastic and reactive dynamics, J. Chem. Phys. **105**, 7864 (1996).